Evaluation of fish-injury mechanisms during exposure to turbulent shear flow

Zhiqun Deng, Gregory R. Guensch, Craig A. McKinstry, Robert P. Mueller, Dennis D. Dauble, and Marshall C. Richmond

Abstract: Understanding the factors that injure or kill turbine-passed fish is important to the operation and design of the turbines. Motion-tracking analysis was performed on high-speed, high-resolution digital videos of juvenile salmonids exposed to a laboratory-generated shear environment to isolate injury mechanisms. Hatchery-reared fall chinook salmon (*Oncorhynchus tshawytscha*, 93–128 mm in length) were introduced into a submerged, 6.35-cm-diameter water jet at velocities ranging from 12.2 to 19.8 m·s^{-1}, with a reference control group released at 3 m·s^{-1}. Injuries typical of turbine-passed fish were observed and recorded. Three-dimensional trajectories were generated for four locations on each fish released. Time series of velocity, acceleration, force, jerk, and bending angle were computed from the three-dimensional trajectories. The onset of minor, major, and fatal injuries occurred at nozzle velocities of 12.2, 13.7, and 16.8 m·s^{-1}, respectively. Opercle injuries occurred at 12.2 m·s^{-1} nozzle velocity, while eye injuries, bruising, and loss of equilibrium were common at velocities of 16.8 m·s^{-1} and above. Of the computed dynamic parameters, acceleration showed the strongest predictive power for eye and opercle injuries and overall injury level, and it may provide the best potential link between laboratory studies of fish injury, field studies designed to collect similar data in situ, and numerical modeling.

Résumé : La conception et la gestion des turbines requièrent une compréhension des facteurs qui blessent ou tuent les poissons qui les traversent. Nous avons fait une analyse du suivi du mouvement sur des bandes vidéo digitales à haute vitesse et haute résolution de jeunes salmonidés exposés à des environnements d'arrachement générés en laboratoire afin d'identifier les mécanismes vulnérants. Nous avons placé des saumons quinnat (*Oncorhynchus tshawytscha* de 93–128 mm de longueur) élevés en pisciculture dans un jet d'eau submergé de 6,35 cm de diamètre à des vitesses variant de 12,2–19,8 m·s^{-1}; le groupe témoin a été placé à une vitesse de 3 m·s^{-1}. Nous avons observé et noté des blessures caractéristiques de poissons qui ont traversé des turbines. Nous avons enregistré des trajectoires tridimensionnelles à quatre sites pour chaque poisson relâché, ce qui nous a permis de calculer des séries chronologiques de vitesse, d'accélération, de force, de secousse et d'angle de repli. Les blessures mineures, majeures et mortelles commencent à se manifester aux vitesses respectives de la lance d'eau de 12,2, 13,7 et 16,8 m·s^{-1}. Des blessures aux opercules se produisent aux vitesses de la lance de 12,2 m·s^{-1}, alors que les blessures aux yeux, les meurtrissures et la perte d'équilibre sont courantes aux vitesses égales et supérieures à 16,8 m·s^{-1}. Parmi les variables dynamiques calculées, l'accélération possède le pouvoir de prédiction le plus élevé pour les blessures aux yeux et aux opercules et pour le niveau global de blessures; elle fournit peut-être le meilleur lien potentiel entre les études des blessures des poissons en laboratoire, les études de terrain qui cherchent à obtenir des données semblables in situ et les modèles numériques.

[Traduit par la Rédaction]

Introduction

Despite advances in turbine design, dam operations, and juvenile fish bypass systems, turbine passage and spillway passage persist as sources of injury and mortality to downstream-migrating salmonids and other fish species in the Columbia River Basin (for overviews, see Coutant and Whitney 2000; Odeh and Sommers 2000; Čada 2001). Dam operators and design engineers are thus faced with the task of making these facilities safer for fish (i.e., more "fish-friendly"), as well as structurally and hydraulically sound and efficient for power generation. To design more fish-friendly facilities, engineers and biologists require reliable estimates of the hydrodynamic forces that fish can withstand.

Development of safer turbines and spillways is currently being approached in three general ways: (*i*) evaluating mortality and injury rates (biological response) in field studies utilizing passive integrated transponder (PIT) tags (CBFWA 1999) and radio-tracking, (*ii*) using laboratory studies to evaluate the physical stresses required to produce the biolog-

Received 13 July 2004. Accepted 10 February 2005. Published on the NRC Research Press Web site at http://cjfas.nrc.ca on 13 July 2005.
J18221

Z. Deng,[1] C.A. McKinstry, R.P. Mueller, D.D. Dauble, and M.C. Richmond. Pacific Northwest National Laboratory, P.O. Box 999, Richland, WA 99352, USA.
G.R. Guensch. Balance Hydrologics, Inc., 841 Folger Avenue, Berkeley, CA 94710, USA.

[1]Corresponding author (e-mail: zhiqun.deng@pnl.gov).

 doi: 10.1139/F05-091

ical responses observed in the field studies, and (*iii*) using reduced-scale physical models and computational fluid dynamics (CFD) modeling techniques to assess design alternatives. Field studies involve tagging fish with radio and balloon tags, releasing them at various locations in the forebay of a dam or turbine intake, recovering them in the tailrace, and documenting their condition (e.g., Mathur et al. 1996, 2000) or using hydroacoustics (Skalski et al. 1996) to monitor passage and inferring passage efficiency (defined as the percentage of fish that pass by a dam by a means other than through the turbines). These types of studies, however, lack a way to determine the specific hydraulic conditions or physical stresses that the fish were exposed to, or the specific causes of the biological response. A promising means of measuring these hydraulic conditions in situ during downstream passage may be the concurrent release of the so-called sensor fish devices equipped to measure and record pressure and acceleration (Carlson and Duncan 2003; Deng et al. 2004). However, unless sensors are installed on the fish themselves, there is no direct way to quantify exactly what pressures, accelerations, or forces a given fish has sustained. One strategy for relating the sensor fish device measurements on the turbine environment to expectations of fish injury rates would be to develop correlation equations from laboratory studies.

Injuries and mortality of fish that pass through hydroelectric turbines can result from several mechanisms, such as rapid and extreme pressure changes, shear stress, turbulence, strike, cavitation, and grinding (Čada 2001). Laboratory studies provide a means of linking the observed biological responses to hydraulic conditions, forces, and stresses that are quantifiable and repeatable. Numerous laboratory studies conducted to date have made substantial progress in quantifying the levels of impact/strike (Turnpenny et al. 1992), shear (Turnpenny et al. 1992; Dauble et al. 2001; Neitzel et al. 2004), pressure (Turnpenny et al. 1992; Abernethy et al. 2001), cavitation (Turnpenny et al. 1992), and turbulence (Odeh et al. 2002) that certain fish can sustain. These data, in turn, have contributed to the development of a promising new generation of more advanced "fish-friendly" turbines, some of which are now being deployed. These advanced turbines typically have smaller gaps, wider leading edges, fewer blades, and redesigned stay vanes (Peltier 2003). Here we attempt to build on this body of data by characterizing the flow field of turbulent shear flows and the fish motion in sufficient detail to facilitate a more fundamental understanding of the mechanics of the injury process and the dynamic variables involved.

Motion tracking from video data is becoming a common experimental tool. Numerous researchers have used video data to study various aspects of swimming fish or their reactions (e.g., Hughes and Kelly 1996; Liao and Lauder 2000; Tang et al. 2000). However, these swimming studies typically do not require exceptionally high camera frame rates. High-speed (500–1000 frames·s^{-1}) video studies of fish tests, especially injury experiments, are less common. Some common high-speed applications of motion-tracking analysis include crash testing in the auto industry (Kang et al. 2001) and studies of impacts and projectile motion (e.g., Hrubes 2001; Tanaka et al. 2002).

The objective of this study was to use high-speed, high-resolution digital cameras and three-dimensional (3D) motion analysis to better quantify the kinematic and dynamic parameters associated with the exposure of fish to turbulent shear flow. The kinematic parameters included the velocity (v), acceleration (a), jerk (J), and bending angle (θ_b) of the fish, while the dynamic parameter was the bulk force (F) on the fish. The injury type and severity were related to fish size (length and mass), exposure strain rate, and magnitude of kinematic and dynamic parameters computed from video-derived 3D trajectory paths.

Methods

Test fish

We tested subyearling fall chinook salmon (*Oncorhynchus tshawytscha*) from stocks originating at the Priest Rapids Hatchery in Washington State in mid- to late September 2003. The test fish were around 7 months old and ranged from 93 to 128 mm in length and from 8.1 to 23.5 g in mass. All test fish were in good to excellent condition prior to testing, in presmolt stage, and actively migrating.

Test facility

A rectangular flume containing a submerged water jet was used to create a quantifiable shear environment consistent with conditions expected within a hydroelectric turbine. The flume was 9 m long, 1.2 m wide, and 1.2 m deep when filled with water. A conical stainless-steel nozzle was bolted to a flange inside the flume at one end. The nozzle began at a diameter of 25.4 cm, constricted to a 6.35-cm diameter over a length of 50.8 cm, and terminated through a tube 4.5 cm long and 6.35 cm in diameter (Fig. 1). A flow conditioner was incorporated upstream of the nozzle to reduce inlet turbulence. Nozzle velocities in excess of 20 m·s^{-1} were achievable with a centrifugal pump with a programmable electronic speed controller.

Fish were actively introduced into the jet through a polycarbonate introduction tube (60 cm long × 3.18 cm in diameter) with a 0.81 m·s^{-1} velocity. The tube was fastened above the nozzle at an angle of 30° (Fig. 1). The terminus of the introduction tube was positioned above and in front of the terminus of the nozzle, with only a 1-cm vertical gap to ensure that test fish contacted the jet. The introduction flow was necessary to ensure that fish passed the terminus of the introduction tube smoothly. Fish were exposed to the following water jet velocities: 3.0 (reference control), 12.2, 13.7, 15.2, 16.8, 18.3, and 19.8 m·s^{-1}.

Fish exposures to the water jet were digitally recorded through viewing windows located on the side and bottom of the flume. The velocity field was characterized using a laser Doppler velocimeter. Neitzel et al. (2000, 2004) contains more detailed information on tank/pump specifications and velocity and turbulence characterization.

Fish handling

To re-identify individual fish during the post-test monitoring, each fish was fitted with a PIT tag prior to testing. The PIT tags (AVID/Destron-Fearing TX1400ST, 12 mm long, 134.2 kHz; Biomark Inc., Boise, ID 83714) were inserted following the protocols outlined in the PIT Tag Mark-

Fig. 1. Nozzle, introduction tube, coordinate system, and a test fish being released. Note that the *y* axis is essentially directed into the page.

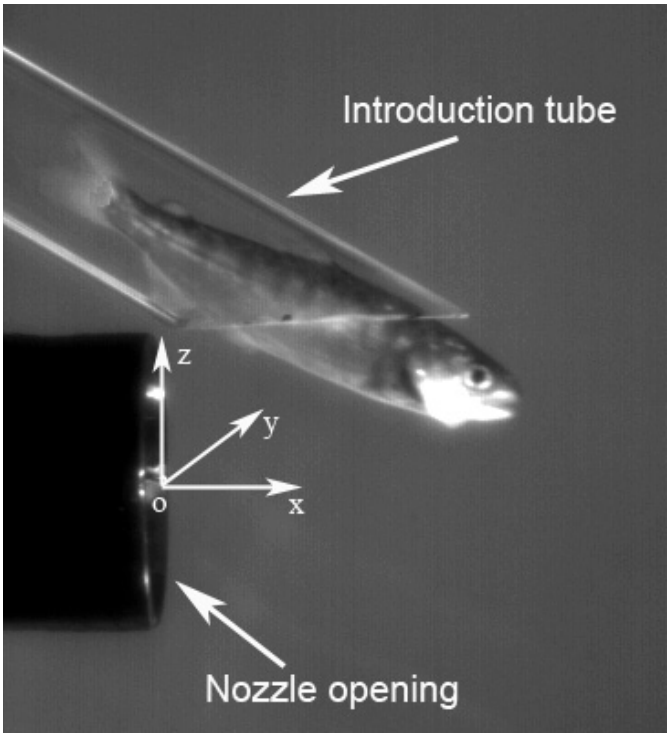

ing Procedures Manual (CBFWA 1999). Fish were anesthetized in 40 mg·L^{-1} MS-222 (3-aminobenzoic acid ethyl ester) solution in a water bath held to a constant temperature (14 °C). Immediately after being tagged, each fish was weighed and measured and its tag was read with a portable Destron-Fearing 2001F PIT tag reader. Fish were allowed a 5-day recovery period before being tested.

Test fish were held near the test facility at low densities in a 1700-L trough with a high water turnover rate. The test flume and holding trough were supplied with 16–17 °C well water. For each test, a fish was randomly captured from the holding trough using a small dip net and scanned with the portable PIT tag transceiver. The unique PIT tag code was recorded and then the fish was placed into a section of clear tubing (cartridge) containing a small volume of water. Each fish was then transferred to the introduction tube, held in the tube until the jet stabilized, and then introduced into the flow field of the jet with the injection flow. The duration of the injection was about 1 s, and the entire deployment and exposure process took less than 20 s.

Within about 10 s following each individual exposure, the pump was turned off and fish were captured from the flume with dip nets. Swimming impairments such as loss of equilibrium, lethargy, and disorientation were evaluated based on the swimming behavior during recapture.

Injury characterization

After recapture, each fish was examined to assess the type and severity of the external injuries (i.e., biological responses) sustained and the direct mortality (immediate and delayed). Following injury evaluation, the fish were photographed and placed in small cages located in the holding trough. Each test group (including reference control fish) was held for 96 h to monitor delayed mortality or other effects indicative of stress or injury (e.g., dark discoloration, lethargy, loss of equilibrium, fungal/disease infection, and osmoregulation problems).

Injury categories included eye damage, descaling, gill/operculum damage, isthmus damage, split fins, bruising/discoloration, and spinal fracture. Disorientation and loss of equilibrium, characterized by reduced swimming ability, were also considered indicators of potentially severe injury and impairment. All these injuries are externally visible injuries and may or may not be indicative of other injuries.

Injury levels similar to those used in Neitzel et al. (2000, 2004) were assigned values from 0 to 4 according to the following criteria: (0) no injury, no observable physical injury or brief minor disorientation; (1) single minor injury, visible but not life-threatening injuries, such as minor bruising, operculum damage, slight gill bleeding, minor isthmus tear, minor descaling, or temporary disorientation; (2) multiple minor injuries, more than one minor injuries but not life threatening; (3) major injury, life-threatening injuries such as severe bruising, bleeding, tearing, creasing, multiple injuries, or prolonged swimming impairment, disorientation, and loss of equilibrium; and (4) mortality, immediate or delayed mortality.

These injury-level and injury-type data were recorded for each fish released and were compiled into a table with the fish information and the dynamic parameter values.

Video recording and processing

Video images of exposed fish were captured using two identical high-speed digital cameras (Photron PCI FastCAM 1280; Photron USA, Inc., San Diego, Calif.) equipped with 50-mm lenses. The cameras captured side (*X–Y* plane) and bottom (*X–Z* plane) views through polycarbonate viewing windows in the side and bottom of the tank. Halogen lamps were used to provide the desired illumination and a gray-colored back panel was used to provide optimal contrast. The cameras recorded fish orientation and location from the moment a fish descended the introduction tube and contacted the shear environment until it was swept out of the immediate shear environment (~0.5 m) downstream. An entire exposure sequence lasted only a fraction of a second. The two cameras recorded each event simultaneously at 1000 frames·s^{-1}. Cameras were focused using a high-contrast resolution target positioned along the axis of the nozzle. Calibration of the field of view for fish metrics was accomplished by using the outer diameter of the nozzle.

The trajectories of four separate points on each fish (nose, head, centroid, and tail) were manually tracked frame by frame in a motion-tracking software package (Visual Fusion® 4.2; Dr. Jack Sanders-Reed, Boeing-SVS Inc., Albuquerque, New Mexico). The side and bottom view tracks were then combined to form a 3D trajectory from which time series of the velocity, acceleration, jerk, bending, and force magnitudes were calculated. These higher-order variables were computed from data smoothed using a 5-point boxcar average. Finally, the average and peak values of each variable were computed for each time series and used in the analysis.

Table 1. Summary of the sample characteristics for each nozzle velocity, where *U*, *L,* m, and IL denote the nozzle velocity, length, mass, and injury level, respectively.

Nozzle velocity, U (m·s^{-1})	Mean fish length, $\bar{L}$ (mm)	Fish length variance, σ_L (mm)	Mean fish mass, $\bar{m}$ (g)	Fish mass variance, σ_m (g)	Mean injury level, $\overline{\text{IL}}$[a]	Injury level variance, σ_{IL}[a]
3.0	112.9	8.69	16.5	3.67	0.1	0.30
12.2	111.4	6.31	15.8	3.65	0.43	0.60
13.7	107.0	9.15	14.0	4.13	1	0.72
15.2	113.0	8.24	15.9	3.67	1.24	0.46
16.8	111.2	7.30	15.4	3.31	1.73	0.57
18.3	108.0	7.79	14.1	3.29	2.36	0.57
19.8	112.2	7.00	15.5	3.38	2.24	0.78

[a]Unitless.

Data analysis

Kinematic and dynamic parameters

The kinematic and dynamic parameter time series were computed from the change in the *x*, *y*, *z* position of the centroid of the fish for each successive time step (Fig. 1). Only random errors associated with motion analysis were considered based on the assumption that the systematic errors were relatively small in comparison. To reduce random errors, the position data were smoothed with a simple 5-point running average prior to the computation of higher-order parameters. Given an assumed maximum random error of one pixel in each direction associated with the motion analysis methodology, the related random errors for other parameters were then estimated. The errors for velocity (*v*), acceleration (*a*), jerk (*J*), and force (*F*) are 0.253 m·s^{-1}, 50.6 m·s^{-2}, 10120 m·s^{-3}, and 0.759 N, respectively. Simplified expressions for each variable are shown in eqs. 1–5 below.

$$(1)\qquad v = \begin{pmatrix} \mathrm{d}x/\mathrm{d}t \\ \mathrm{d}y/\mathrm{d}t \\ \mathrm{d}z/\mathrm{d}t \end{pmatrix}$$

$$(2)\qquad a = \mathrm{d}v/\mathrm{d}t$$

$$(3)\qquad J = \mathrm{d}a/\mathrm{d}t$$

$$(4)\qquad F = \mathrm{m}\cdot a$$

$$(5)\qquad \theta_{\mathrm{b}} = \arccos\left(\frac{A^2 + B^2 - C^2}{2AB}\right)$$

where *m* is the fish mass, d*t* is the time step (equal to the time between digitized frames, 0.001 s), and changes in variables between successive digitized frames are indicated by the differential (d). For example, $\mathrm{d}x = x_i - x_{i-1}$, where *i* indicates the frame number. The values *A*, *B*, and *C* are the three sides of a triangle formed by the bent fish, where *A* and *B* are the sides formed by the fish body and *C* is the side connecting the head and tail (opposite to θ_{b}). The peak value of each dynamic parameter for each release was used in the subsequent statistical analysis.

Statistical analysis

The five-level scale classifications of observed fish injuries were used to define binomial response variables for different levels and types of injury. Binary injury responses were fit to the set of peak dynamic parameters in separate logistic regression models of the form shown in eq. 6.

$$(6)\qquad p(x) = \frac{\mathrm{e}^{\mathbf{X}\boldsymbol{\beta}}}{1 + \mathrm{e}^{\mathbf{X}\boldsymbol{\beta}}}$$

where $p(x)$ is the expected probability of a fish sustaining a specified level or type of injury, $\boldsymbol{\beta}$ is the vector of fitted coefficients, and $\mathbf{X}$ is the model matrix. Confidence intervals at the 95% level were computed as well.

Model selection was performed using a sequential analysis of deviance approach (McCullagh and Nelder 1989) to arrive at the most parsimonious set of kinematic and dynamic parameters in the final model. Individual parameters were entered into the model in descending order of deviance as computed from a univariate logistic regression of each parameter on the binary response. Since overdispersion was evident in the data, the more conservative *F* test was used at each model-building step to assess model improvement and account for lack of fit.

Using logistic regression in this way, a functional relationship was established between the expected biological injury rate and a subset of the most predictive kinematic and dynamic parameters. Binary responses were defined for minor or worse injury, major or worse injury, eye damage, and operculum damage.

Results

Biological response

Twenty-one fish were released headfirst at each nozzle velocity (3.0, 12.2, 13.7, 15.2, 16.8, 18.3, and 19.8 m·s^{-1}). The basic characteristics of each group (summarized in Table 1) show that the groups did not differ significantly in mass or length. They also show that the mean injury level for each group increased with increasing nozzle velocity up to 18.3 m·s^{-1} and then decreased slightly at 19.8 m·s^{-1}. This decrease was within the uncertainty range of the data as estimated by the sample standard deviations.

Minor injuries occurred at the lowest nozzle velocity, 12.2 m·s^{-1}, and in two reference control fish. Appreciable levels (38%) of major injury occurred at 13.7 m·s^{-1}. Substantial total mortality (14%) occurred at 16.8 m·s^{-1} (Fig. 2). Mortality within 1 h following exposure was first observed at 16.8 m·s^{-1} and increased to nearly half of the fish tested at 18.3 and 19.8 m·s^{-1}. Fewer additional mortalities occurred at

Fig. 2. Summary of injury levels at each nozzle velocity (n = 21 for all nozzle velocities). Minor injury, hatched bars; major injury, stippled bars; 1-h mortality, open bars; 24-h mortality, shaded bars; total mortality, solid bars.

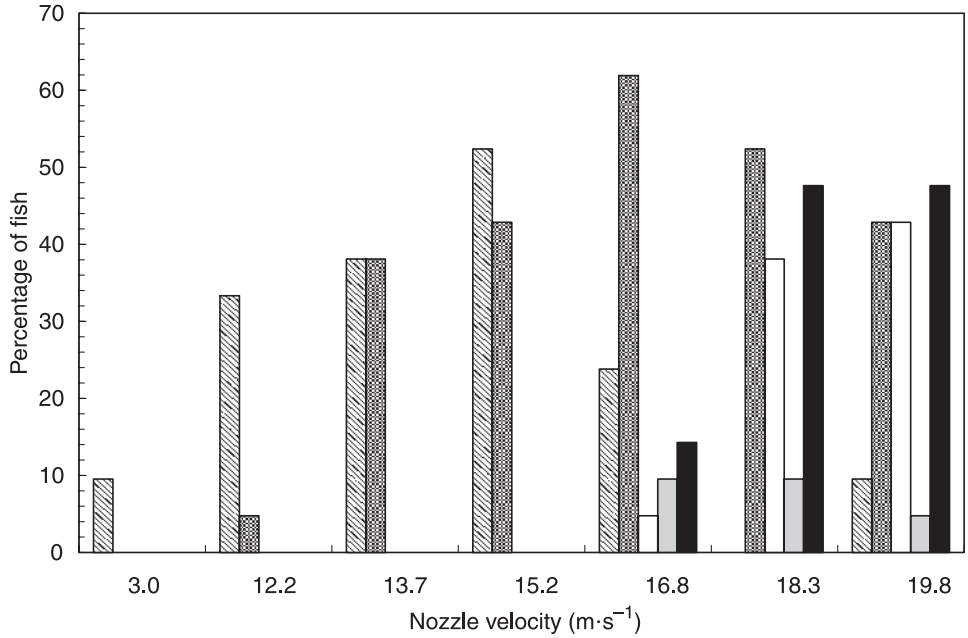

Fig. 3. Example of inverted opercle from fish released at 19.8 m·s^{-1}.

Table 2. Pairwise correlation between nozzle velocity, acceleration, and jerk of fish and force sustained by fish.

Velocity			
0.829	Acceleration		
0.695	0.876	Force	
0.817	0.843	0.741	Jerk

24 h and none occurred at 96 h (Fig. 2). Injuries to the operculum (Fig. 3) occurred in 70%–90% of the fish tested at nozzle velocities of 15.2 m·s^{-1} or greater, making the operculum the most commonly injured organ. Eye damage, bruising, and loss of equilibrium occurred in 40%–50% of the fish released at nozzle velocities of 16.8 m·s^{-1} and above (Fig. 4).

Motion analysis results

Motion analysis results computed from the fish tracks for three nozzle velocities, 3 m·s^{-1} (reference control), 13.7 m·s^{-1} (low speed), and 18.3 m·s^{-1} (high speed), show the general pattern of each parameter (Fig. 5). At the point of entrainment into the jet, the three groups differ substantially, with the exception of downstream distance (x) for the low- and high-speed releases (Fig. 5*a*). Generally, the high-speed release sustained the most severe exposure to all the parameters and the reference control fish experienced the least (Figs. 5*b*–5*f*). Estimates of jerk were very high for the non-control groups, especially for the high-speed release group, and very sensitive to changes in acceleration (Fig. 5*d*). The net force on the body of the fish differs from the acceleration by a constant factor, the fish mass (Figs. 5*c* and 5*e*). Bending angle, the interior angle of the fish as it exited the tube (e.g., 180° means the fish is straight and 0° means the fish is folded in half), was most severe at 40° for the fish released at a high nozzle velocity (Fig. 5*f*).

Statistical analysis results

Pairwise correlations showed high levels of positive correlation between nearly all the variables (Table 2). This was largely because all kinematic and dynamic parameters were computed from the same video-derived frame-to-frame displacements. Force and velocity were least correlated, whereas force and acceleration, as expected, were most correlated.

The high degree of correlation between the kinematic and dynamic parameters (Table 3) preclude incorporation of

Fig. 4. Summary of different injury types at each nozzle velocity (n = 21 for each nozzle velocity). Eye damage/loss, solid bars; opercle damage, open bars; bruised, shaded bars; loss equilibrium/lethargy, hatched bars.

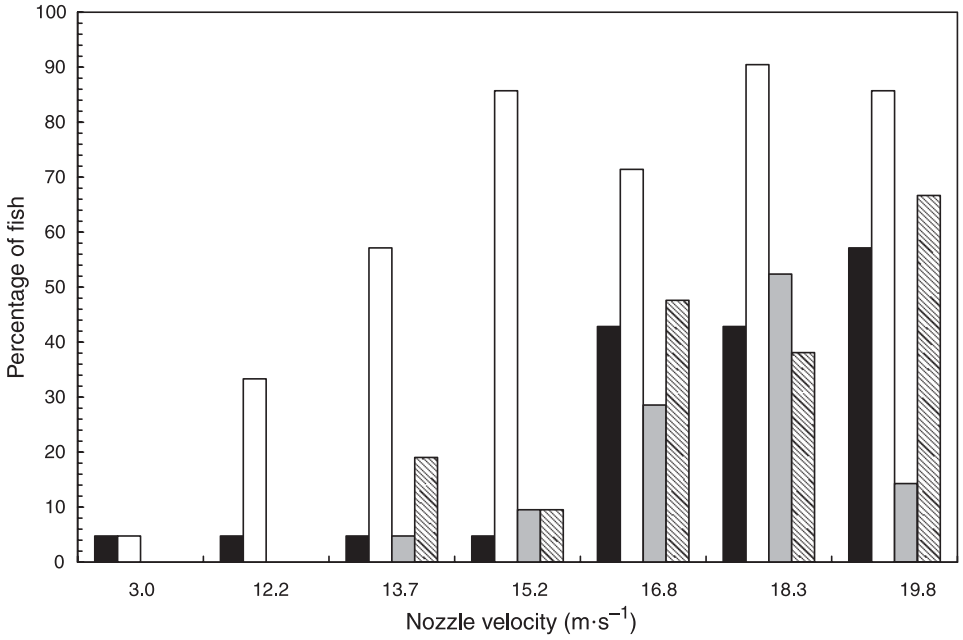

Table 3. Univariate modeling correlations between incidence of injury and kinematic and dynamic parameters from logistic regression of individual fish injury levels.

	df	Deviance	Residual df	Residual deviance	F value	Pr(F)
Velocity	1	67.38	143	99.43	73.16	<0.001
Acceleration	1	74.56	143	92.25	85.87	<0.001
Force	1	59.21	143	107.60	43.75	<0.001
Jerk	1	59.09	143	107.72	46.80	<0.001

Table 4. Analysis of deviance ordered by univariate model results from logistic regression of individual fish injury levels.

	df	Deviance	Residual df	Residual deviance	F value	Pr(F)
Null			144	166.81		
Acceleration	1	74.56	143	92.25	87.38	<0.001
Velocity	1	2.26	142	89.99	2.64	0.106
Force	1	0.00	141	89.99	0.00	0.988
Jerk	1	0.21	140	89.78	0.25	0.618

more that just acceleration into the binomial model. Sequential construction of the model in this fashion controls for these high correlations between candidate model predictor variables (Table 4). Because acceleration showed the highest predictive power of the binary injury variables, it was entered first into the model, followed by velocity, force, and jerk. However, none of the additional variables showed significant improvement in model fit over the model containing acceleration.

The results of the binomial logistic regression relate the probability of specific biological responses to acceleration (Fig. 6). The probability of minor injury or worse increased quickly starting at 100 m·s^{-2} and reaching nearly 1.0 by 900 m·s^{-2} (Fig. 6*a*). The probability of major injuries was similarly shaped to that for minor injuries but was increased by roughly 200 m·s^{-2} towards higher accelerations (Fig. 6*b*). The expected probabilities of an eye (Fig. 6*c*) or operculum (Fig. 6*d*) injury were similar and increased slowly at low acceleration levels and became linear beyond 700 m·s^{-2} (Figs. 6*c* and 6*d*).

Discussion

Thresholds of injury

The onset of injury or biological response at or above the 10% level was used to indicate threshold levels of parameters evaluated in this study. Our tests showed the onset of minor, major, and fatal injuries to occur at nozzle velocities of 12.2, 13.7, and 16.8 m·s^{-1}, respectively. Injuries associated with the operculum were most common at all nozzle velocities and were the only injuries to occur at significant levels at the lowest test jet velocity of 12.2 m·s^{-1}. Loss of

Fig. 5. Examples of motion analysis results of fish releases at three nozzle velocities (only one out of 21 releases per nozzle velocity is plotted) for the bulk kinematic/dynamic parameters: (*a*) streamwise location (*x*); (*b*) velocity (*v*); (*c*) acceleration (*a*); (*d*) jerk (*J*); (*e*) force (*F*); (*f*) bending angle (θ_b). Velocities: 3 m·s^{-1}, broken line; 13.7 m·s^{-1}, solid squares; 18.3 m·s^{-1}, open circles.

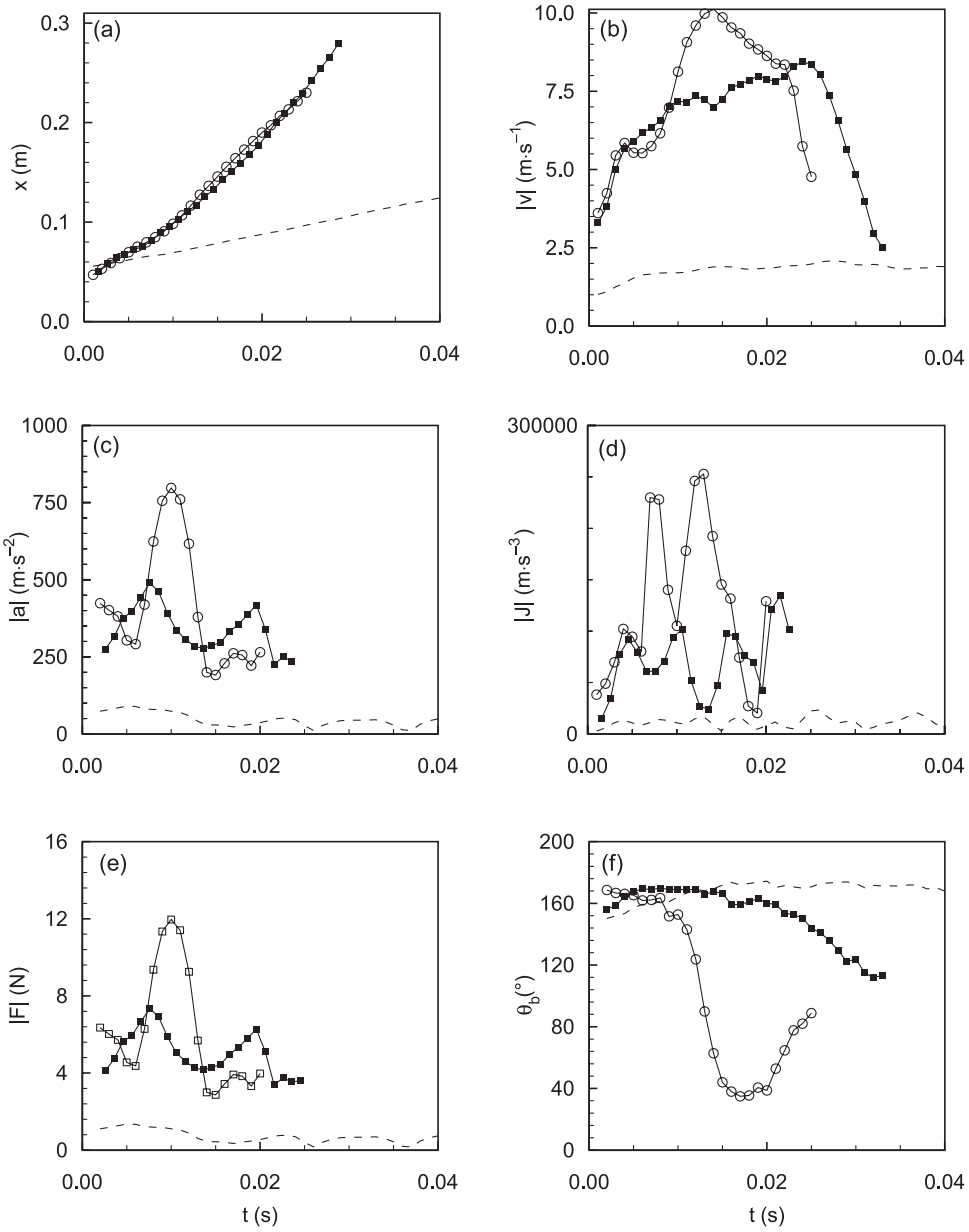

equilibrium occurred in more than 10% of fish, at the next highest nozzle velocity of 13.7 m·s^{-1}, although it decreased to 9% at 15.2 m·s^{-1}. Eye damage, bruising, and loss of equilibrium all became clearly prevalent at 16.8 m·s^{-1}.

These results can be compared, either directly or through simple conversions, to those reported by other investigators. Neitzel et al. (2000, 2004) conducted similar tests and expressed the jet severity in terms of exposure strain rate (s^{-1}), which was essentially the fluid strain rate computed at the scale of a test fish (i.e., jet velocity/approximate width of a test fish). Converting our critical jet velocities in this manner gives key exposure strain rates of 677, 761, and 933 s^{-1} for minor, major, and fatal injuries, respectively. Our exposure strain rate value of 677 s^{-1} for the onset of minor injuries corresponds well to the 683 s^{-1} value documented by Neitzel et al. (2000, 2004). Turnpenny et al. (1992) also conducted similar experiments and noted the onset of severe eye and operculum injuries to occur at a shear stress level of 1920 N·m^{-2}, which corresponds to a jet velocity of 15 m·s^{-1} and an exposure strain rate of ~833 s^{-1}, which is within range of our results.

In contrast to jet velocity and exposure strain, which basically represent flow-field characteristics, the kinematic and dynamic parameters determined from motion tracking were specific to each individual fish. Of these parameters, acceleration of the fish correlated most strongly with fish injury. Threshold or critical levels of fish acceleration were also determined based on the probability of injury as a continuous function of the acceleration of the fish. For example, the 0.1, or 10%, probability of minor, major, eye, and operculum in-

Fig. 6. Fitted probability of four types of injury as a function of acceleration, with 95% predictive confidence intervals (broken lines), as derived from binary logistic regression: (*a*) minor; (*b*) major; (*c*) eye; (*d*) operculum.

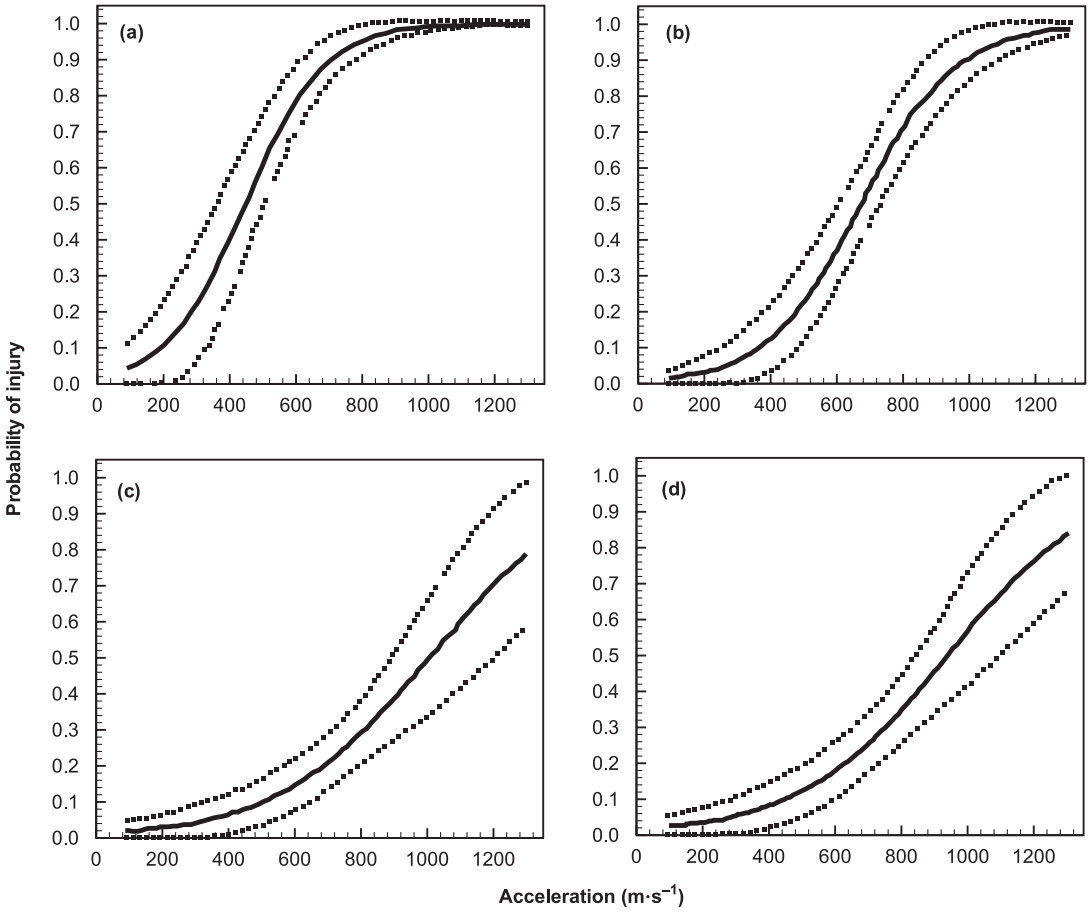

Table 5. Accelerations (m·s^{-2}) of fish corresponding to injury probabilities of 5%, 10%, and 15% with 95% confidence intervals in parenthesis.[a]

Injury type	5% (P = 0.05)	10% (P = 0.10)	15% (P = 0.15)
Minor injury	100 (0–280)	180 (20–310)	240 (140–350)
Major injury	240 (90–380)	340 (210–440)	360 (250–460)
Eye	300 (80–520)	500 (310–640)	600 (360–710)
Opercle	250 (90–490)	440 (270–600)	550 (390–670)

[a]For example, 10% probability of major injuries corresponds to fish acceleration level of 340 m·s^{-2}, with the lower and upper curves bounding the 95% confidence interval being 210 m·s^{-2} and 440 m·s^{-2}, respectively.

juries corresponds to fish acceleration levels of 180, 340, 500, and 440 m·s^{-2}, respectively. Ranges for these estimates were determined based on the lower and upper curves bounding the 95% confidence interval (Table 5).

The relationships described here between fish injury and either exposure strain rate or acceleration will be most effectively used in combination with information on what passing fish are actually exposed to. Particle tracking algorithms within CFD models (Richmond et al. 2004) or accelerations measured in the field with a sensor fish (Carlson and Duncan 2003) are two possible sources of exposure information. For example, one could use the relationships presented here to estimate probability of injury from CFD-derived estimates of the exposure strain rate or the acceleration to which particles are exposed, greatly enhancing the potential to use CFD as a biohydraulic design tool. Similarly, the acceleration time series measured in the field with the sensor fish device (Carlson and Duncan 2003) could be converted to a time series of fish injury probability using the probability of injury versus fish acceleration relationship, which would enhance the effectiveness of the sensor fish device as an assessment tool. These new and innovative approaches will gradually come to fruition over the next few years as CFD modeling capabilities improve and the sensor fish device is refined.

Mechanics of injury

The vulnerability of fish to injury in turbulent shear flows is best understood in terms of fish physiology and the resulting stresses on the fish. Salmonids are evolutionarily adapted

for swimming head-on into the flow. In this orientation, they are streamlined to minimize drag, can tolerate extremely severe velocities, velocity changes, or accelerations, and can even use shear stresses and turbulence to their advantage (Vogel 1996; Liao et al. 2003). They are poorly adapted, however, to flow coming from behind. Such reverse flows can lift and tear off scales, pry open the operculum, rupture or dislodge eyes, and damage gills.

The opercula are most vulnerable to damage from reverse flow, as observed here, because they are easily pried open and then flare out and act as a parachute or spinnaker, essentially capturing the energy contained in a disproportionately large area of flow. This parachute effect increases drag and accelerates the fish faster than if it were oriented head-on to the flow field. Most importantly, however, the anatomical shape and structure is such that the stress is focused on the two small attachment points of each operculum—the upper left and right attachment points on the head, and the shared lower attachment point at the isthmus. A pushing or pressure force applied to the entire operculum is transmitted to the fish as a tensile stress focused at these pin-sized attachment points, in a manner somewhat analogous to tearing a partially torn piece of paper or breaking a v-notched shaft.

Value of kinematic and dynamic approachs in a hydraulic environment

Our study suggests that fish injuries were proportional to the velocity of flow field and also subject to stochastic factors acting in combination, such as the orientation of the body and vulnerable anatomy of the fish when it encounters the water jet, the reaction of the fish, and the characteristics of the water jet at the instant of contact. The stochastic component is evidenced by the slightly reduced average injury level for the group released at the highest nozzle velocity (e.g., 19.8 $m \cdot s^{-1}$), an observation for which there was no other defensible explanation, and the large standard deviation in injury levels for each jet velocity. This stochasticity can make simple relationships between flow field characteristics, such as velocity and shear, and biological response misleading. The use of kinematic and dynamic parameters overcomes this problem because they describe the actual motion of each individual fish and, therefore, more effectively account for the stochastic variations. When incorporated into an empirical modeling approach, as shown here, these kinematic and dynamic parameters are more robust predictors of fish injury. Further, these kinematic and dynamic parameters are more suitable for comparison with sensor fish data and CFD particle-tracker output.

The approach described here to estimate the bulk kinematic motion and mechanical force sustained by a fish in a hydraulic environment is also more applicable to turbine passage than measuring forces and stresses directly and then attempting to translate them to a hydraulic environment. More accurate measures of the forces on specific organs would be possible using direct mechanical means (e.g., Geerlink and Videler 1987; Long 1992; Miller 2001) instead of the in situ method used here. Direct forces, however, would be difficult to apply in a manner relevant to what a fish experiences in a hydraulic environment. Also, precise mechanical measures of localized yield strength of specific parts of individual organs such as operculum or eyes may not be useful to turbine designers at the present time, because such fine-scale phenomena are not typically available from CFD turbine models used in design or field studies. Currently, the best method of assessing fluid-induced forces is to measure them in the fluid environment as shown here or, alternatively, by using force measurement tools such as tensiometers and force transducers. Forces and stresses measured this way can be related to information incorporated into models used in turbine design, such as velocity distributions, strain rates, shear stresses, turbulence, and possibly particle acceleration if used with a particle-tracking routine.

In summary, a number of basic conclusions can be drawn from this study. The onset of minor, major, and fatal injuries occurred at 12.2, 13.7, and 16.8 $m \cdot s^{-1}$ jet velocities, respectively. These jet velocities correspond to exposure strain rates of 677, 761, and 933 s^{-1}, which agree with previous experiments. Motion-tracking analysis provides a means of measuring the bulk kinematics, forces, and deformations sustained by fish in experimental hydraulic environments. The kinematic and dynamic parameters that can be computed from the motion-tracking data (v, a, F, J, and θ_b) incorporate some of the inherent stochasticity of the fish releases and, therefore, can be more rigorously related to biological response than parameters based solely on simple jet characteristics. The bulk acceleration of the fish was most predictive of all injury types and overall injury level. The predictive power of force would probably be stronger if a broader range of fish body masses were tested. Acceleration is a more convenient parameter than force in some respects because it can be compared directly with both CFD output and field-derived sensor fish data.

Acknowledgments

This work was conducted at the Pacific Northwest National Laboratory (PNNL) in Richland, Washington. We thank Tom Giever and Jessica Vucelick at PNNL for their field and laboratory support. Battelle Memorial Institute operates PNNL for the US Department of Energy. We thank Jim Ahlgrimm from the US Department of Energy for his leadership and support of this research.

References

Abernethy, C.S., Amidan, B.G., and Čada, G.F. 2001. Laboratory studies of the effects of pressure and dissolved gas supersaturation on turbine-passed fish. US Department of Energy, Idaho Operations Office, Idaho Falls, Idaho, Paper No. DOE/ID-10853.

Čada, G.F. 2001. The development of advanced hydroelectric turbines to improve fish passage survival. Fisheries, **26**(9): 14–23.

Carlson, T.J., and Duncan, J.P. 2003. Evolution of the sensor fish device for measuring physical conditions in severe hydraulic environments. Pacific Northwest National Laboratory, Richland, Wash., Paper No. DOE/ID-11079.

Columbia Basin Fish and Wildlife Authority (CBFWA). 1999. PIT tag marking procedures manual. Published by PIT Tag Operations Center (PTOC), Portland, Oregon.

Coutant, C.C., and Whitney, R.R. 2000. Fish behavior in relation to passage through hydropower turbines: a review. Trans. Am. Fish. Soc. **129**: 351–380.

Dauble, D.D., Neitzel, D.A., Richmond, M.C., Carlson, T.J., Mueller, R.P., and Guensch, G.R. 2001. Design guidelines for

high flow smolt bypass outfalls: field, laboratory, and modeling studies. Pacific Northwest National Laboratory, Richland, Wash., Paper No. PNNL-13608.

Deng, Z., Richmond, M.C., Simmons, C.S., and Carlson, T.J. 2004. Six degrees of freedom sensor fish design: governing equations and motion modeling. Pacific Northwest National Laboratory, Richland, Wash., Paper No. PNNL-14779.

Geerlink, P.J., and Videler, J.J. 1987. The relation between structure and bending properties of teleost fin rays. Neth. J. Zool. **37**(1): 59–80.

Hrubes, J.D. 2001. High-speed imaging of supercavitating underwater projectiles. Exp. Fluids, **30**: 57–64.

Hughes, N.F., and Kelly, L.H. 1996. New techniques for video tracking of fish swimming movements in still or flowing water. Can. J. Fish. Aquat. Sci. **53**: 2473–2483.

Kang, J., Agaram, V., Nusholtz, G., and Kostyniuk, G. 2001. Air bag loading on in-position Hybrid III dummy neck. Society of Automotive Engineers, Inc., Warrendale, Penn., Paper No. 2001-01-0179.

Liao, J., and Lauder, G.V. 2000. Function of the heteroceral tail in white sturgeon: flow visualization during steady swimming and vertical maneuvering. J. Exp. Biol. **203**: 3585–3594.

Liao, J.C., Beal, D.N., Lauder, G.V., and Triantafyllou, M.S. 2003. The Kármán gait: novel body kinematics of rainbow trout swimming in a vortex street. J. Evol. Biol. **206**: 1059–1073.

Long, J.H., Jr. 1992. Stiffness and damping forces in the intervertebral joints of blue marlin (*Makiaira nigricans*). J. Exp. Biol. **162**: 131–155.

Mathur, D., Heisey, P.G., Euston, E.T., Skalski, J.R., and Hays, S. 1996. Turbine passage survival estimation for chinook salmon smolts (*Oncorhynchus tshawythscha*) at a large dam on the Columbia River. Can. J. Fish. Aquat. Sci. **53**: 542–549.

Mathur, D., Heisey, P.G., Skalski, J.R., and Kenney, D.R. 2000. Salmonid smolt survival relative to turbine efficiency and entrainment depth in hydroelectric power generation. J. Am. Water Resour. Assoc. **36**(4): 737–747.

McCullagh, P., and Nelder, J.A. 1989. Generalized linear models. 2nd ed. Chapman and Hall Inc., New York.

Miller, K. 2001. How to test very soft tissues in extension. J. Biomech. **34**: 651–657.

Neitzel, D.A., Richmond, M.C., Dauble, D.D., Mueller, R.P., Moursund, R.A., Abernethy, C.S., Guensch, G.R., and Čada, G.F. 2000. Laboratory studies on the effects of shear on fish: final report. Pacific Northwest National Laboratory, Richland, Wash., Paper No. PNNL-13323.

Neitzel, D.A., Dauble, D.D., Cada, G.F., Richmond, M.C., Guensch, G.R., Mueller, R.P., Abernethy, C.S., and Amidan, B.G. 2004. Survival estimates for juvenile fish subjected to a laboratory-generated shear environment. Trans. Am. Fish. Soc. **133**: 447–454.

Odeh, M., and Sommers, G. 2000. New design concepts for fish friendly turbines. Int. J. Hydropower Dams, **7**(3): 64–71.

Odeh, M., Noreika, J.F., Haro, A., Maynard, A., Castro-Santos, T., and Cada, G.F. 2002. Evaluation of the effects of turbulence on the behavior of migratory fish. Final Report to Bonneville Power Administration, Contract No. 00000022, Project No. 200005700 (BPA Report DOE/BP-00000022-1).

Peltier, R.P. 2003. Fish-friendly turbines move center stage. Power, **147**(3): 37–43.

Richmond, M.C., Carlson, T.J., Serkowski, J.A., Cook, C.B., and Duncan, J.P. 2004. Characterizing the fish-passage environment at the Dalles Dam spillway. *In* Proceedings of 2004 World Water and Environmental Resources Congress, Salt Lake City, Utah. American Society of Civil Engineers (ASCE), Reston, Virginia.

Skalski, J.R., Johnson, G.E., Sullivan, C.M., Kudera, E., and Erho, M.W. 1996. Statistical evaluation of turbine bypass efficiency at Wells Dam on the Columbia River, Washington. Can. J. Fish. Aquat. Sci. **53**: 2188–2198.

Tanaka, K., Nishida, M., Kunimochi, T., and Takagi, T. 2002. Discrete element simulation and experiment for dynamic response of two-dimensional granular matter to the impact of a spherical projectile. Powder Technology, **124**: 160–173.

Tang, M., Bosclair, D., Ménard, C., and Downing, J.A. 2000. Influence of body weight, swimming characteristics, and water temperature on the cost of swimming in brook trout (*Salvelinus fontinalis*). Can. J. Fish. Aquat. Sci. **57**: 1482–1488.

Turnpenny, A.W.H., Davis, M.H., Fleming, J.M., and Davies, J.K. 1992. Experimental studies relating to the passage of fish and shrimps through tidal power turbines. Marine and Freshwater Biology Unit, National Power, Fawley, Southampton, Hampshire, England.

Vogel, S. 1996. Life in moving fluids: the physical biology of flow. Princeton University Press, Princeton, N.J.